

MECHANICAL CHARACTERIZATION AND MICROMECHANICAL MODELING OF WOVEN CARBON/COPPER COMPOSITES¹

BRETT A. BEDNARCYK² and Marek-Jerzy Pindera³
University of Virginia
Charlottesville, VA

David L. Ellis and Robert V. Miner
NASA Lewis Research Center
Cleveland, OH

Introduction

In recent years, interest in woven and braided composites has been on the rise. These materials consist of reinforcing fibers, or bundles of fibers called yarns, woven or braided into a desired preform prior to consolidation with traditional matrix materials. Woven and braided composites offer excellent out-of-plane impact and crack resistance while possessing far superior stability during manufacture compared to their traditional counterparts, Fig. 2.

The present investigation examines the in-plane mechanical behavior of a particular woven metal matrix composite (MMC); 8-harness (8H) satin carbon/copper (C/Cu). This is accomplished via mechanical testing as well as micromechanical modeling, Fig. 1. While the literature is replete with experimental and modeling efforts for woven and braided polymer matrix composites, little work has been done on woven and braided MMCs (ref. 1). Thus, the development and understanding of woven MMCs is at an early stage. 8H satin C/Cu owes its existence to the high thermal conductivity of copper and low density and thermal expansion of carbon fibers. It is a candidate material for high heat flux applications, such as space power radiator panels.

The experimental portion of this investigation consists of monotonic and cyclic tension, compression, and Iosipescu shear tests, as well as combined tension-compression tests. Tests were performed on composite specimens with three copper matrix alloy types: pure Cu, Cu-0.5 weight percent Ti (Cu-Ti), and Cu-0.7 weight percent Cr (Cu-Cr). The small alloying additions are present to promote fiber/matrix interfacial bonding (ref. 2, 3). The analytical modeling effort utilizes an approach in which a local micromechanical model is embedded in a global micromechanical model. This approach differs from previously developed analytical models for woven composites in that a true repeating unit cell is analyzed. However, unlike finite element modeling of woven composites, the geometry is sufficiently idealized to allow efficient geometric discretization and efficient execution.

Material System

Six plates with each matrix type were produced via pressure infiltration casting. The reinforcement phase was provided by Amoco, and it consisted of three layers of VCX-11 carbon fiber yarns woven in the 8H pattern (Fig. 3). The Cr and Ti matrix alloying additions have been shown to locate preferentially at fiber/matrix interfaces in C/Cu composites, allowing reaction and a superior bond (ref. 3). Fig. 4a

¹ Work funded under NASA Grant NAG3-1319.

² Ph.D. Candidate.

³ Associate Professor.

shows an optical micrograph of a typical plate cross-section. Note the presence of porosity within the infiltrated fiber yarns (Fig. 4b).

Experimental Results

Fig. 5 shows the results of a typical monotonic tension test and a typical monotonic compression test on 8H satin C/Cu. The tensile response of the copper matrix and the carbon fiber (longitudinal and transverse) are included for comparison. In tension, the composite typically exhibited little elastic behavior and stiffened noticeably at higher strains. Failure in tension occurred by fracture of the matrix, leaving fiber yarns intact across the failure surface. In compression, the composite did not stiffen and failed at a lower stress and strain compared to tension. Failure occurred via microbuckling of the layers of the woven reinforcement. The apparent stiffer initial response in the compressive test compared to the tensile test (Fig. 5) is believed to be an artifact of the different specimens and test fixtures used in the different tests.

The effect of matrix alloy type on the monotonic tensile and compressive response of 8H satin C/Cu is shown in Fig. 6. Recall that the matrix alloying elements were added to improve fiber/matrix interfacial bonding, with the C/Cu-Cr composite possessing the best interfacial bond, followed by C/Cu-Ti, and finally by C/Cu. In tension, the observed trend in the three stress-strain curves is opposite that expected. That is, C/Cu-Cr, with its superior fiber-matrix bonding, would be expected to have the stiffest overall response, followed by C/Cu-Ti, and finally by C/Cu, which is not the case. In compression, on the other hand, the observed trend in the stress-strain curves follows the expected trend. Future work will attempt to explain these trends via detailed micromechanical modeling. Note in Fig. 6 that a greater amount of stiffening occurred in the alloyed-matrix composites compared to the C/Cu composite.

Fig. 7 shows the results of typical cyclic tension tests for composites with each matrix alloy type. Large amounts of hysteresis were present upon unloading for both the C/Cu-Cr and C/Cu composites. Examining the loading and unloading elastic modulus for each cycle revealed that the hysteresis is not caused by damage within the composite (ref. 1). It is believed that the hysteresis is caused by kinematic hardening of the matrix and frictional effects associated with sliding along the poorly-bonded fiber/matrix interface. The results of typical shear tests on 8H satin C/Cu composites with each alloy type are shown in Fig. 8. As was the case in compression, the shear stress-strain curves exhibited the trend expected based on the interfacial bond strength.

Model Results and Correlation

The model developed for this investigation consists of the original method of cells micromechanics model (ref. 4) embedded in the three-dimensional generalized method of cells (GMC-3D) micromechanics model (ref. 5) (Fig. 9). This embedded approach allows the global three-dimensional geometry of the woven composite to be represented by GMC-3D, while the local behavior of the infiltrated fiber yarns is modeled by the original method of cells. Matrix plasticity is included on the local level.

The simplest geometric representation of the repeating unit cell for an 8H satin woven composite is shown in Fig. 10a. Fig. 10b shows the next level of refinement in which the yarn cross-over regions are more accurately represented. The results presented herein are preliminary, generated using the simple geometry. Fig. 11 compares the predictions of the model with actual data from tension tests. Predictions are presented for the fully infiltrated case as well as the case in which the infiltrated fiber yarns contain 14% (by volume) porosity. Although experimental results for all three matrix alloy types are included,

the model results should be compared with the C/Cu-Cr results since the present model treats the fiber and matrix as well-bonded. Hence, even when porosity is included the model overpredicts the tensile response of 8H satin C/Cu. Fig. 12 compares model predictions with the compressive response of the composite. In this case the model underpredicts the composite response, and inclusion of porosity degrades the correlation. Fig. 13 shows that in shear, the model significantly overpredicts the response of the composite. It is likely that the absence of fiber/matrix debonding in the model, which is probably present even in the C/Cu-Cr composite, accounts for a good deal of the discrepancy between the model and experiment. Other sources of the discrepancy include the coarse unit cell geometry used in the micromechanical model, and the absence of residual stresses from fabrication cool down.

Conclusions

The mechanical response of 8H satin C/Cu has been characterized via mechanical testing and micromechanical modeling. Tensile testing of the composite revealed a small elastic range, noticeable stiffening at higher strains, and large hysteresis loops upon unloading. The stiffening behavior has been attributed to straightening of the fiber yarns, while the hysteresis has been attributed to kinematic hardening of the matrix and frictional effects associated with the fiber/matrix interface. In tension, failure occurred by fracture of the matrix with the fiber yarns remaining intact. In compression, failure occurred via microbuckling, resulting in a lower ultimate strength and strain to failure than in tension, Fig. 14.

Comparing results for the three copper matrix alloy types with different degrees of fiber/matrix bonding showed that in tension, the observed trend in stress-strain curves is opposite to that expected. In compression and shear, however, the expected trend was observed. The unexpected behavior in tension may be due to a complex interaction of the microstructural architecture of the cross-over regions, fiber/matrix debonding, and residual stresses. These will be addressed in the future (Fig. 15, 16). Modeling the response of the composite was performed using a local/global embedding approach which allows an accurate yet efficient representation of the composite geometry. The model-experiment correlation was reasonably good for tension and compression, but poor for shear. Future work will involve improving this correlation via inclusion of fiber/matrix debonding, as well as other effects, in the model (Fig. 16), and utilizing a more refined unit cell geometry (Fig. 10b).

References

1. Bednarczyk, B.A.; Pauly, C.C.; and Pindera, M.-J.: Experimental Characterization and Micromechanical Modeling of Woven Carbon/Copper Composites. NASA CR-202318, 1997.
2. Ellis, D.L.: Properties of Graphite Fiber Reinforced Copper Matrix Composites for Space Power Applications. NASA CR-191026, 1992.
3. DeVincent, S.M.: Interfacial Effects on the Thermal and Mechanical Properties of Graphite/Copper Composites. NASA CR-198370, 1995.
4. Aboudi, J.: Micromechanical Analysis of Composites by the Method of Cells. *App. Mech. Reviews*, vol. 42, 1989, pp. 193-221.
5. Aboudi, J.: Micromechanical Analysis of Thermo-Inelastic Multiphase Short-Fiber Composites. NASA CR-195290, 1994.

Objectives

- Characterize the mechanical behavior of 8-harness (8H) satin C/Cu
 - Stress-strain response
 - Identification of factors affecting the behavior
1. Mechanical testing
 - Tension tests (monotonic & cyclic)
 - Compression tests (monotonic & cyclic)
 - Combined tension-compression tests
 - Iosipescu shear tests (monotonic & cyclic)
 2. Micromechanical modeling: Embedded approach
 - Local model: Original Method of Cells
 - Global model: Three-Dimensional Generalized Method of Cells

Fig. 1

Woven Composites → Background

- Reinforcement → fabric woven from fiber or bundles of fibers (yarns)
- Simplifies handling during fabrication → fabric vs. individual fibers
- Near net-shaped woven or braided preforms
- Many different types of weaves:

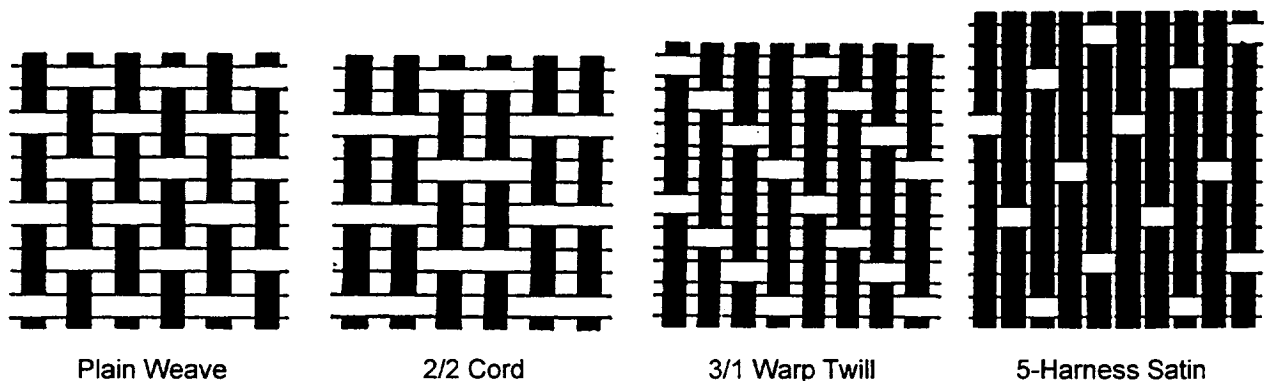


Fig. 2

Material System → 8H Satin C/Cu

- Candidate for high heat flux aerospace applications: space power radiator panels
- 3 layers Amoco VCX-11 carbon fiber yarns of reinforcement woven in 8H satin pattern:

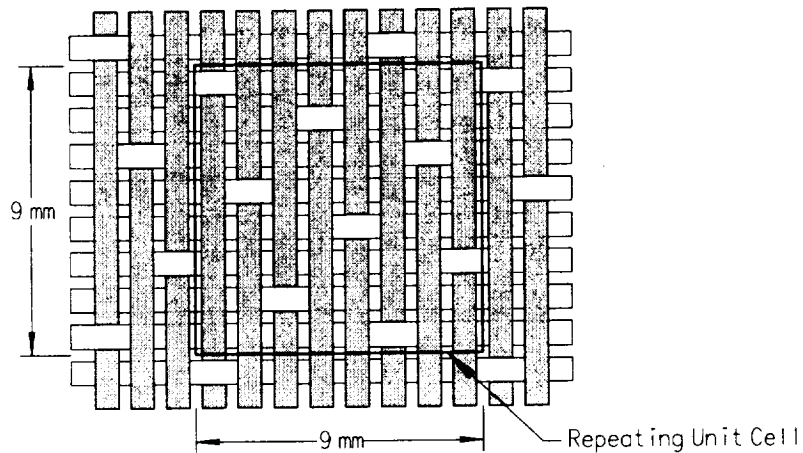


Fig. 3

Material System → 8H satin C/Cu

- Three Cu matrix alloy type: pure Cu, Cu-0.5 wt. % Ti, Cu-0.7 wt. % Cr
- Alloying additions present to improve fiber/matrix bonding, not to affect matrix mechanical properties
- Porosity present within infiltrated fiber yarns:

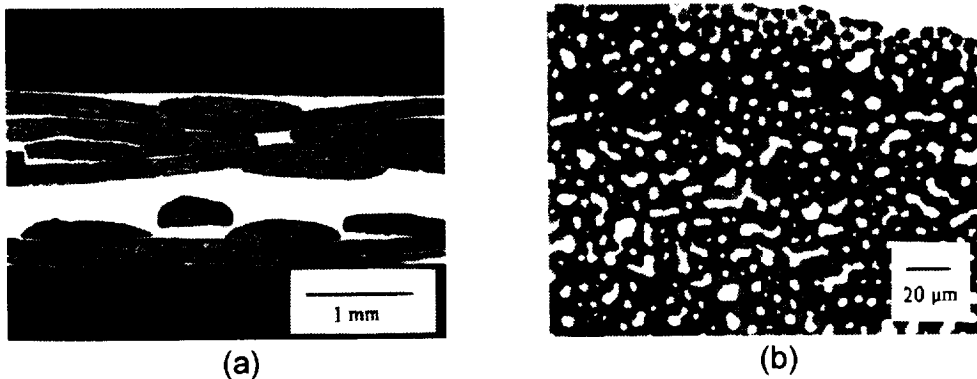


Fig. 4

Experimental Results → Monotonic Tension & Compression

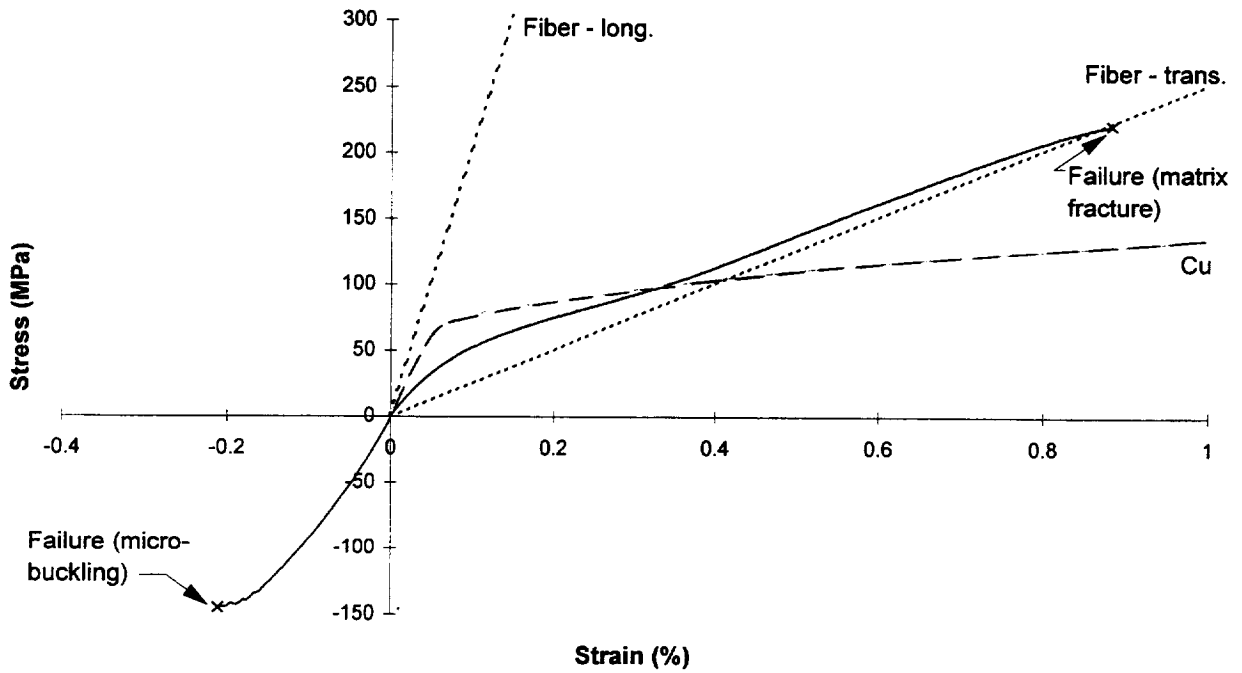


Fig. 5

Experimental Results → Monotonic Tension (Matrix Alloy)

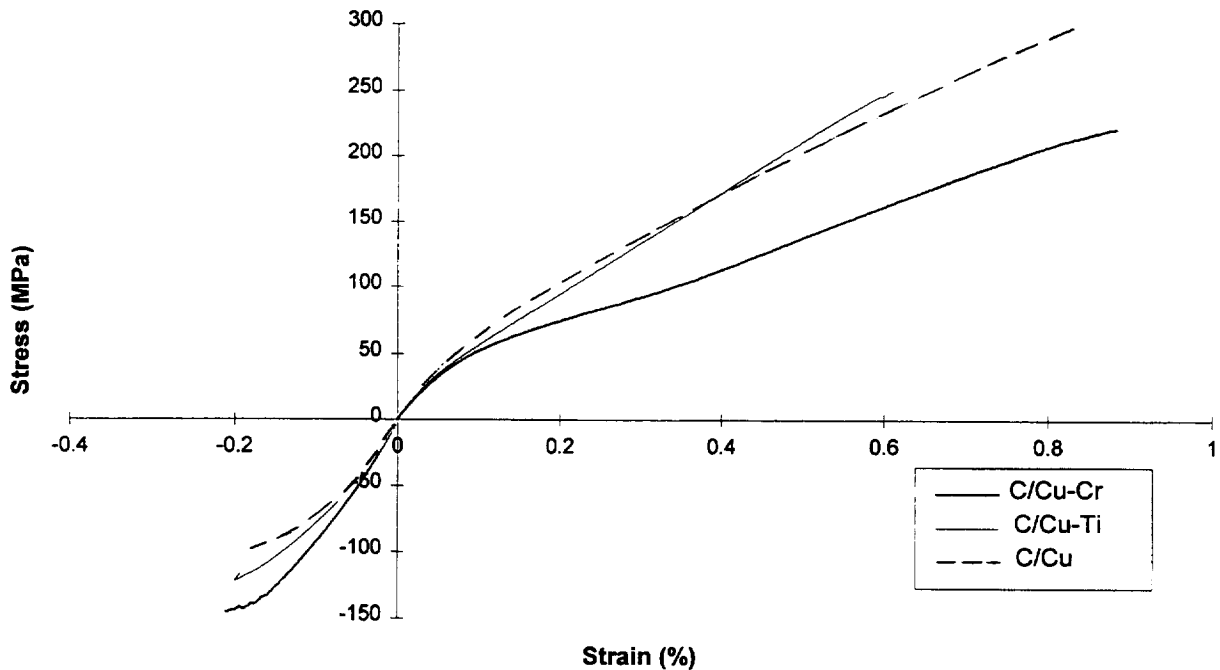


Fig. 6

Experimental Results → Cyclic Tension (Matrix Alloy)

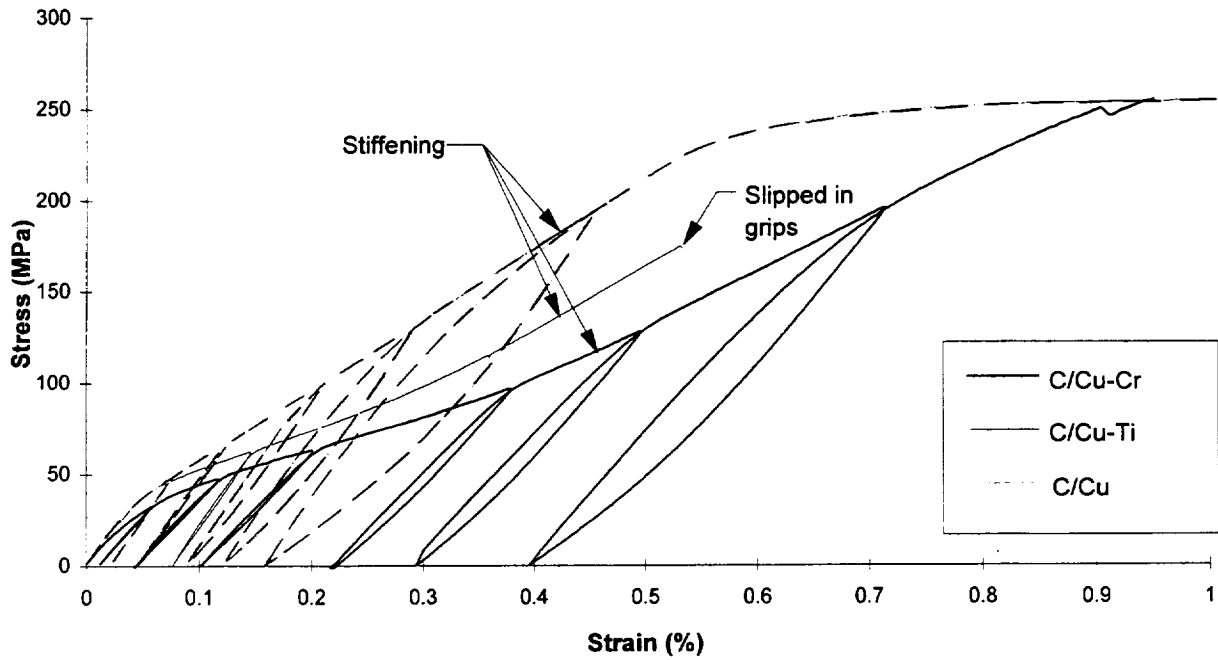


Fig. 7

Experimental Results → Monotonic Shear (Matrix Alloy)

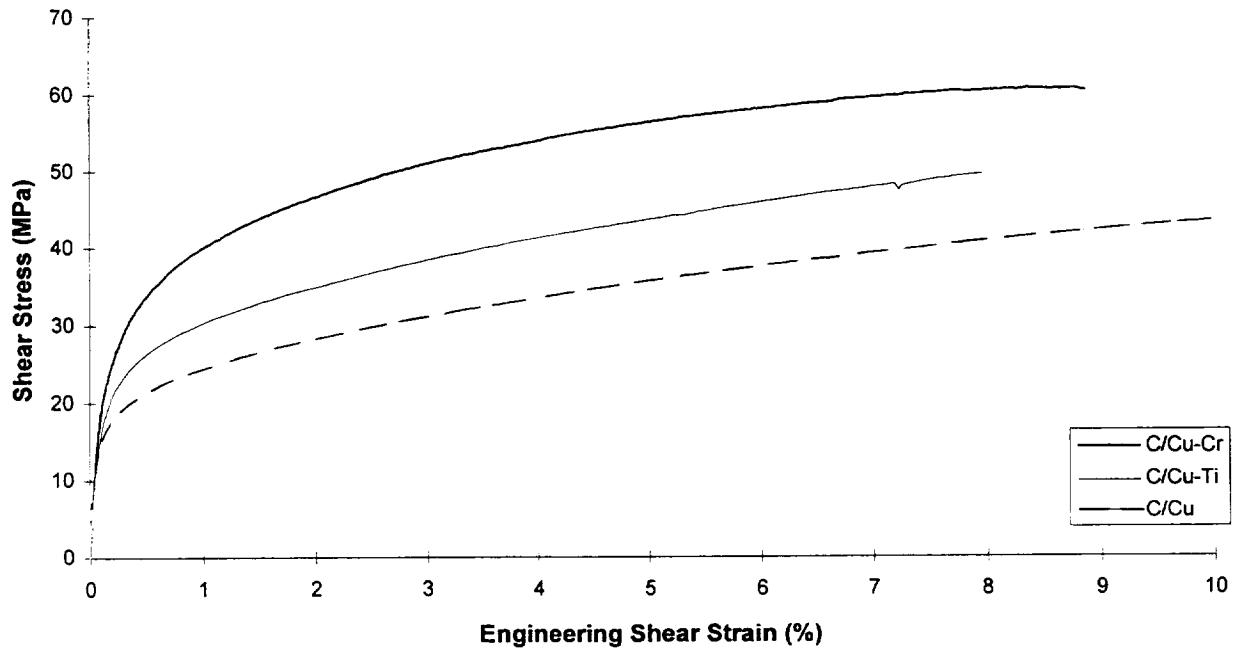


Fig. 8

Micromechanical Model → Approach

- Local model → original method of cells > *embedded* <
- Global Model → GMC-3D

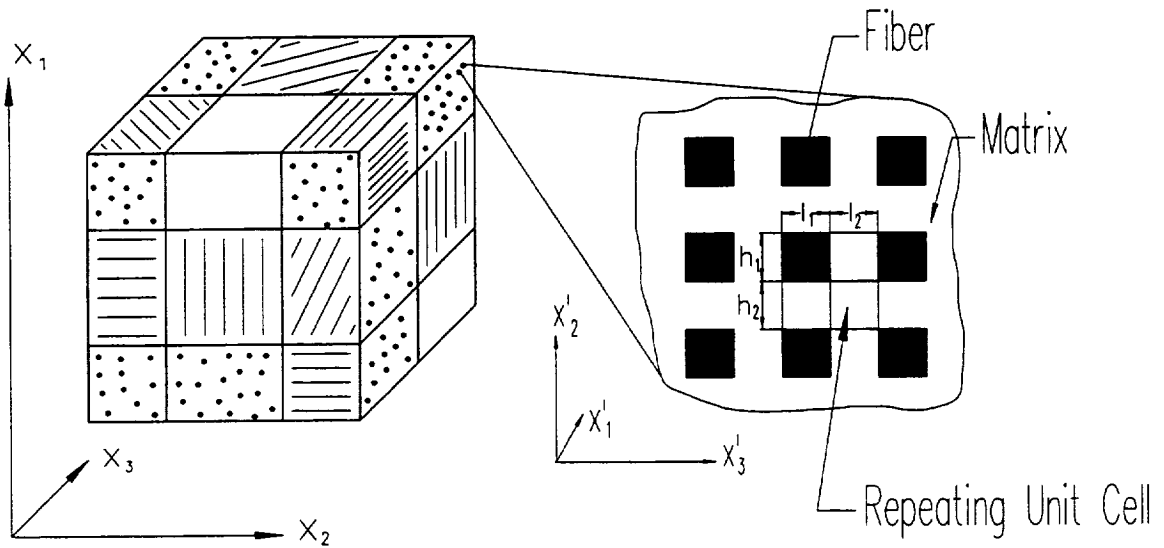


Fig. 9

Micromechanical Model → Repeating Unit Cells

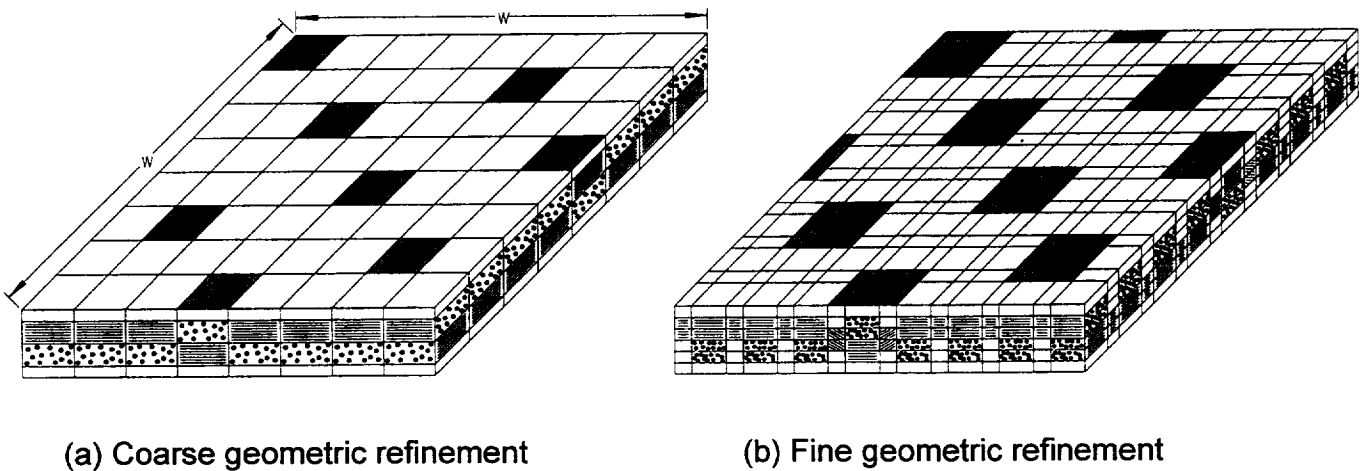


Fig. 10

Model vs. Experiment → Tension

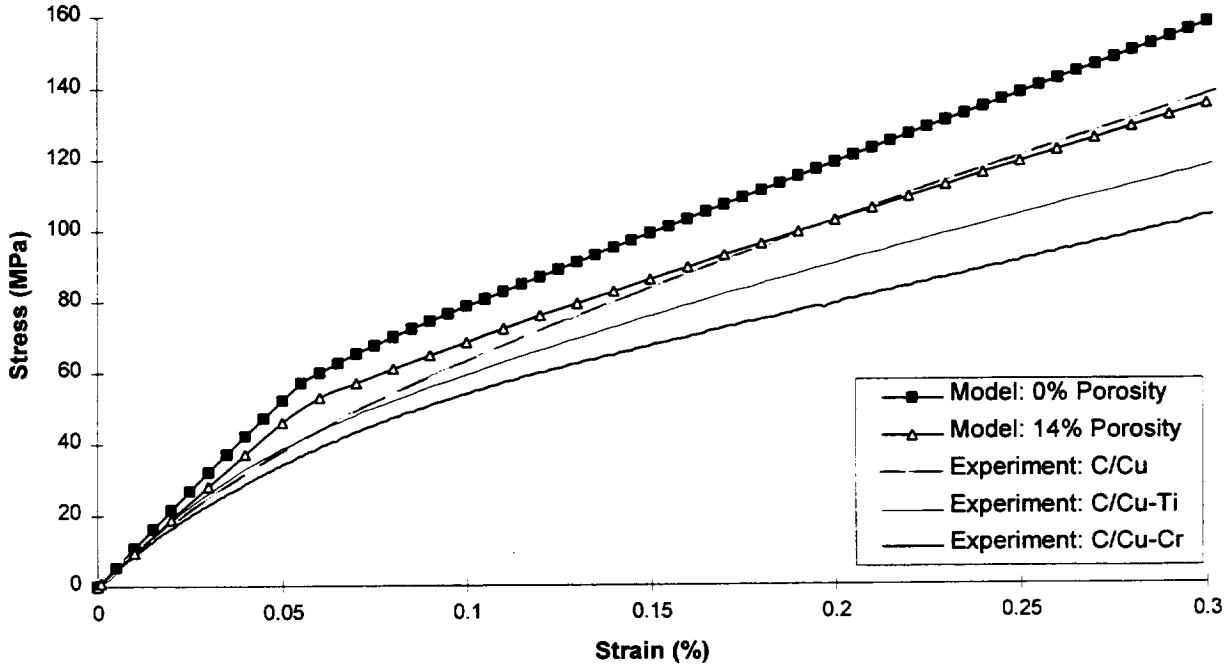


Fig. 11

Model vs. Experiment → Compression

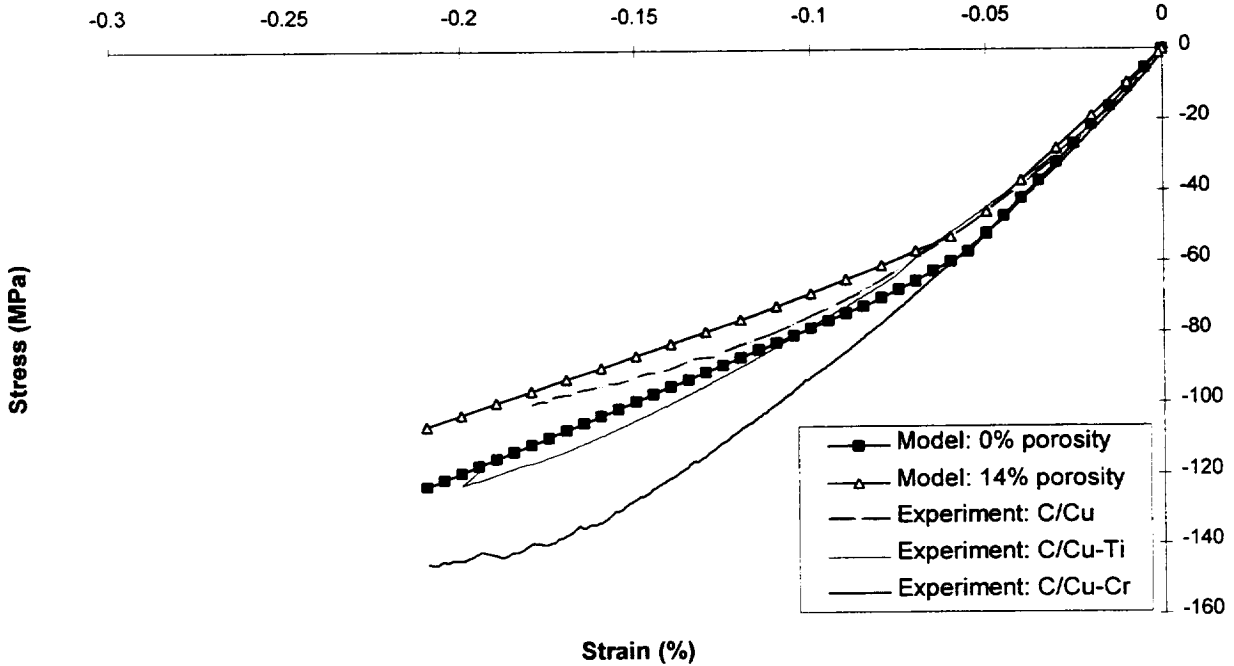


Fig. 12

Model vs. Experiment → Shear

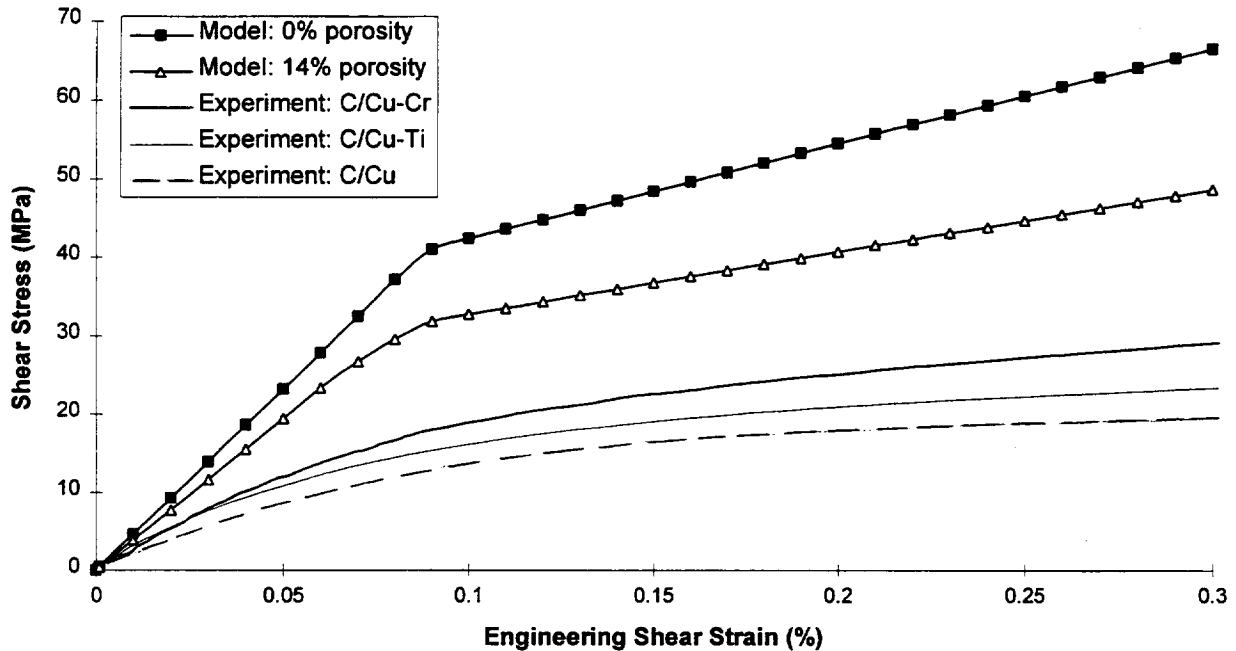


Fig. 13

Summary

- Mechanical behavior of 8H satin C/Cu characterized: three Cu matrix alloys (increasing bond strength): pure Cu → Cu-Ti → Cu-Cr
- Porosity present within infiltrated fiber yarns
- Mechanical testing:
 - Monotonic and cyclic tension, compression, and shear and combined tension-compression tests performed
 - Elastic range small, large amount of inelastic behavior
 - Large amount of hysteresis: kinematic hardening & frictional effects
 - Failure modes, ultimate strength, strain to failure different for tension & compression
- Micromechanical Modeling:
 - Embedded local/global approach
 - Allows representation of true unit cell geometry
 - Plasticity incorporated on level of local model

Fig. 14

Conclusion

- Trend expected based on the fiber/matrix bond strength observed in compression and shear
- Trend opposite to that expected observed in tension
- Model predictions correlate reasonably well in tension and compression
- Model predictions are poor in shear
- To explain unexpected trend based on the fiber/matrix bond strength, and improve the model-experiment correlation, the following factors should be considered:
 - Fiber/matrix debonding
 - Porosity
 - Repeating unit cell geometric refinement
 - Residual stresses
 - Grip constraint effects (compression and combined tests only)

Fig. 15

Future Work

- Include fiber/matrix debonding in model
- Utilize more refined geometry in model
- Model residual stresses
- Model grip constraint effect for compression & combined tests
- Continued analysis of experimental results

Fig. 16

